Electronic Supplementary Material (ESI) for Nanoscale Advances.

Supporting Information

to

Alzheimer's disease-related amyloid β peptide causes structural disordering of lipids and changes the electric properties of a floating bilayer lipid membrane.

Dusan Mrdenovic,[†,§] Zhangfei Su,[§] Wlodzimierz Kutner,[†,‡] Jacek Lipkowski[§,*] Piotr Pieta[†,*]

[†]Institute of Physical Chemistry, Polish Academy of Sciences, Kasprzaka 44,/52, 01-224 Warsaw, Poland

[‡]Faculty of Mathematics and Natural Sciences, School of Sciences, Cardinal Stefan Wyszynski University in Warsaw, Wóycickiego 1/3, 01-815 Warsaw, Poland

[§]Department of Chemistry, University of Guelph, 50 Stone Road East, Guelph, Ontario N1G 2W1, Canada

e-mail address: ppieta@ichf.edu.pl

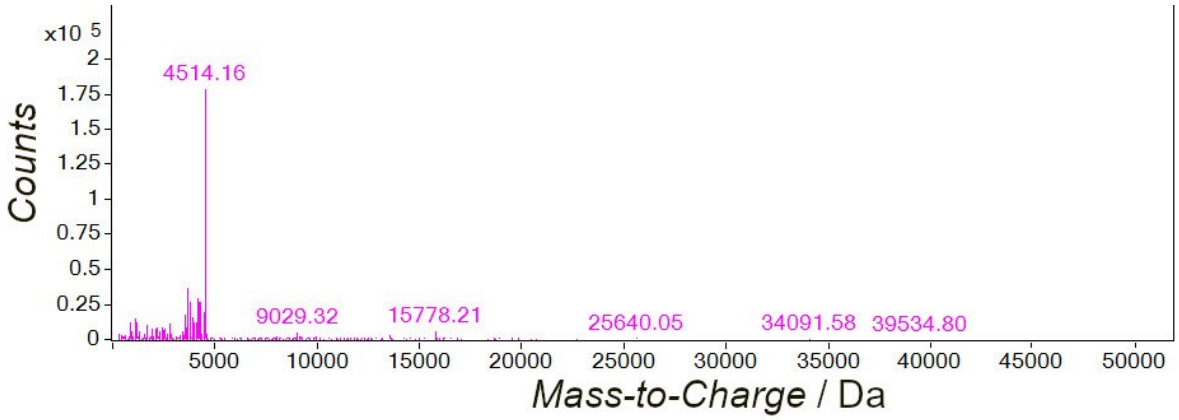

Figure S1. Mass spectrum showing Aβ molecular weight.

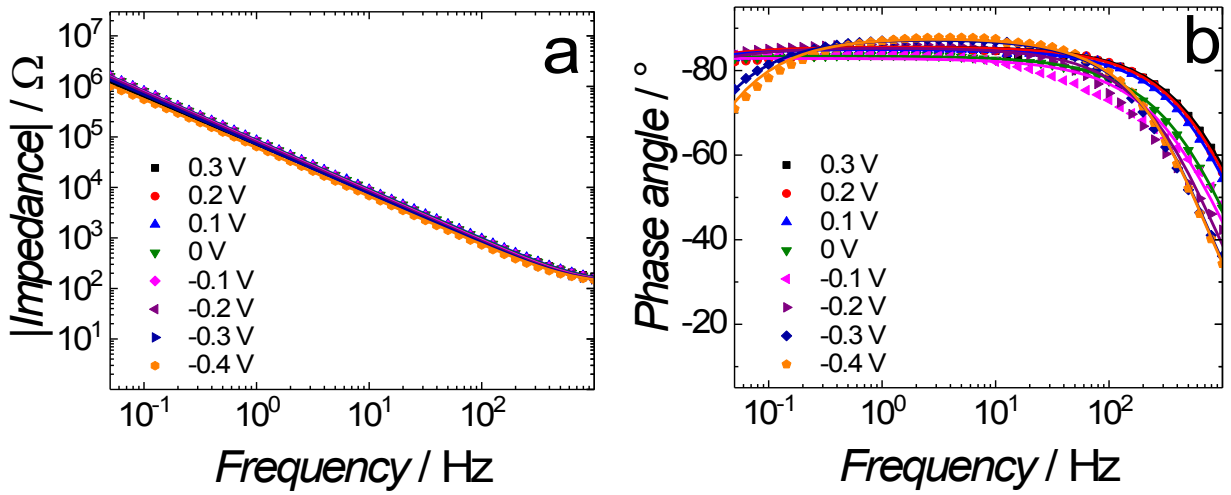

Figure S2. Impedance (a) magnitude and (b) phase angle as a function of frequency for the fBLM. Symbols and curves of the same colors represent experimental data and results of fitting the equivalent electrical circuits to the data, respectively.

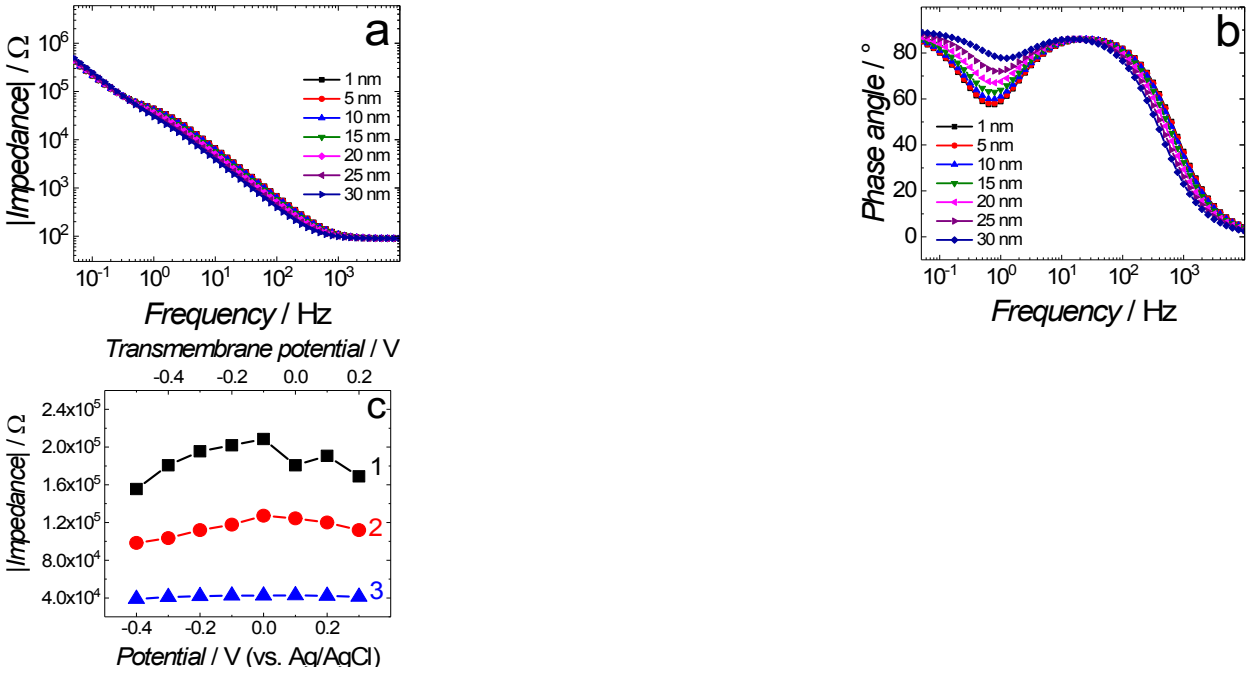

Figure S3. The EIS simulated curves of the (a) impedance and (b) phase angle dependence on frequency for the membrane with pores of different radii. Modeling was performed using the pore radii from 1 to 30 nm. Other parameters are: defect density, N_{def} = 190 μm^{-2}; Helmholtz layer capacitance, C_H = 0.06 F cm^{-2}; membrane capacitance, C_m = 0.045 F cm^{-2}; solution resistance, R_{sol} = 90 Ω; pore conductance, Y_{def} = 0.7 pS; thickness of the submembrane spacer layer, d_{sub} = 1.7 nm; specific resistance of the conducting media in the submembrane spacer layer, ρ_{sub} = 10^5 Ω cm. (c) Experimental impedance as a function of potential

at the phase angle vs. frequency minimum for the fBLM (curve 1), fBLM-AβM (curve 2) and fBLM-AβO (curve 3) in the PBS (0.01 M phosphate buffer, 0.0027 M KCl, and 0.137 M NaCl, pH = 7.4) solution. The upper abscissa plots the transmembrane potential that accounts for the potential of zero free charge (E_{pzfc} = 0.11 V vs. Ag/AgCl).

Table S1. Numerical results of the equivalent electric circuits fittings to the EIS data for fBLM in the Aβ absence (fBLM), fBLM in the presence of Aβ monomers (AβMs) and fBLM in the presence of Aβ oligomers (AβOs) at different potentials in the PBS (0.01 M phosphate buffer, 0.0027 M KCl, and 0.137 M NaCl, pH = 7.4) solution.

E V vs Ag/AgCl	Q_m(fBLM) μF cm^{-2}	Q_m(AβMs) μF cm^{-2}	Q_m(AβOs) μF cm^{-2}	α_m(fBLM)	α_m(AβMs)	α_m(AβOs)	R_m(fBLM) MΩ cm^2	R_m(AβMs) MΩ cm^2	R_m(AβOs) MΩ cm^2	Q_{sp}(AβOs) μF cm^{-2}	α_{sp}(AβOs)
0.3	15.03 ± 0.06	18.19 ± 0.06	20.61 ± 0.08	0.924 ±0.001	0.956 ±0.001	0.941 ±0.006	4.71 ±0.77	1.83 ±0.05	0.0124 ± 0.0001	28.37 ± 0.12	0.927 ± 0.003
0.2	14.14 ± 0.04	15.69 ± 0.04	19.83 ± 0.05	0.930 ±0.002	0.964 ±0.001	0.943 ±0.005	9.42 ±1.78	2.37 ±0.06	0.0127 ± 0.00009	28.17 ± 0.09	0.938 ± 0.002
0.1	13.83 ± 0.05	14.32 ± 0.04	19.68 ± 0.04	0.936 ±0.001	0.968 ±0.001	0.945 ±0.004	11.92 ±2.59	2.77 ±0.07	0.0133 ± 0.00008	26.21 ± 0.07	0.963 ± 0.001
0.0	13.59 ± 0.04	14.18 ± 0.03	19.67 ± 0.04	0.951 ±0.001	0.974 ±0.001	0.946 ±0.003	12.01 ±1.63	2.892 ±0.07	0.0131 ± 0.00007	25.37 ± 0.07	0.969 ± 0.001
-0.1	13.31 ± 0.03	14.64 ± 0.03	20.12 ± 0.05	0.963 ±0.002	0.970 ±0.001	0.946 ±0.004	11.71 ±0.83	2.75 ±0.06	0.0135 ± 0.00009	26.01 ± 0.08	0.964 ± 0.002
-0.2	13.69 ± 0.02	15.29 ± 0.04	20.75 ± 0.05	0.967 ±0.002	0.969 ±0.001	0.946 ±0.004	6.60 ±0.17	2.15 ±0.04	0.0134 ± 0.00008	29.24 ± 0.08	0.935 ± 0.002
-0.3	14.69 ± 0.04	16.54 ± 0.06	21.64 ± 0.07	0.968 ±0.001	0.965 ±0.001	0.945 ±0.006	2.881 ±0.05	0.980 ±0.02	0.0130 ± 0.0001	33.87 ± 0.13	0.898 ± 0.003
-0.4	16.72 ± 0.08	19.26 ± 0.14	23.07 ± 0.13	0.972 ±0.002	0.957 ±0.002	0.944 ±0.009	1.193 ±0.01	0.331 ±0.01	0.0119 ± 0.0002	41.01 ± 0.26	0.845 ± 0.005

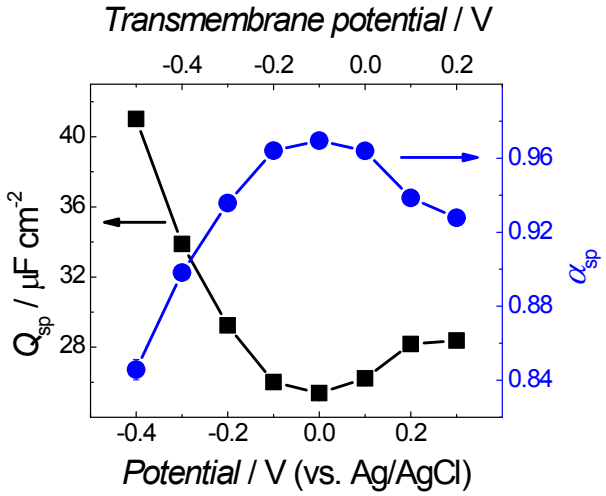

Figure S4. The constant phase element, Q_{sp}, and α_{sp} coefficient, representing impedance of the spacer layer as a function of electrode potential for the fBLM with AβO in the PBS (0.01 M phosphate buffer, 0.0027 M KCl, and 0.137 M NaCl, pH = 7.4) solution.

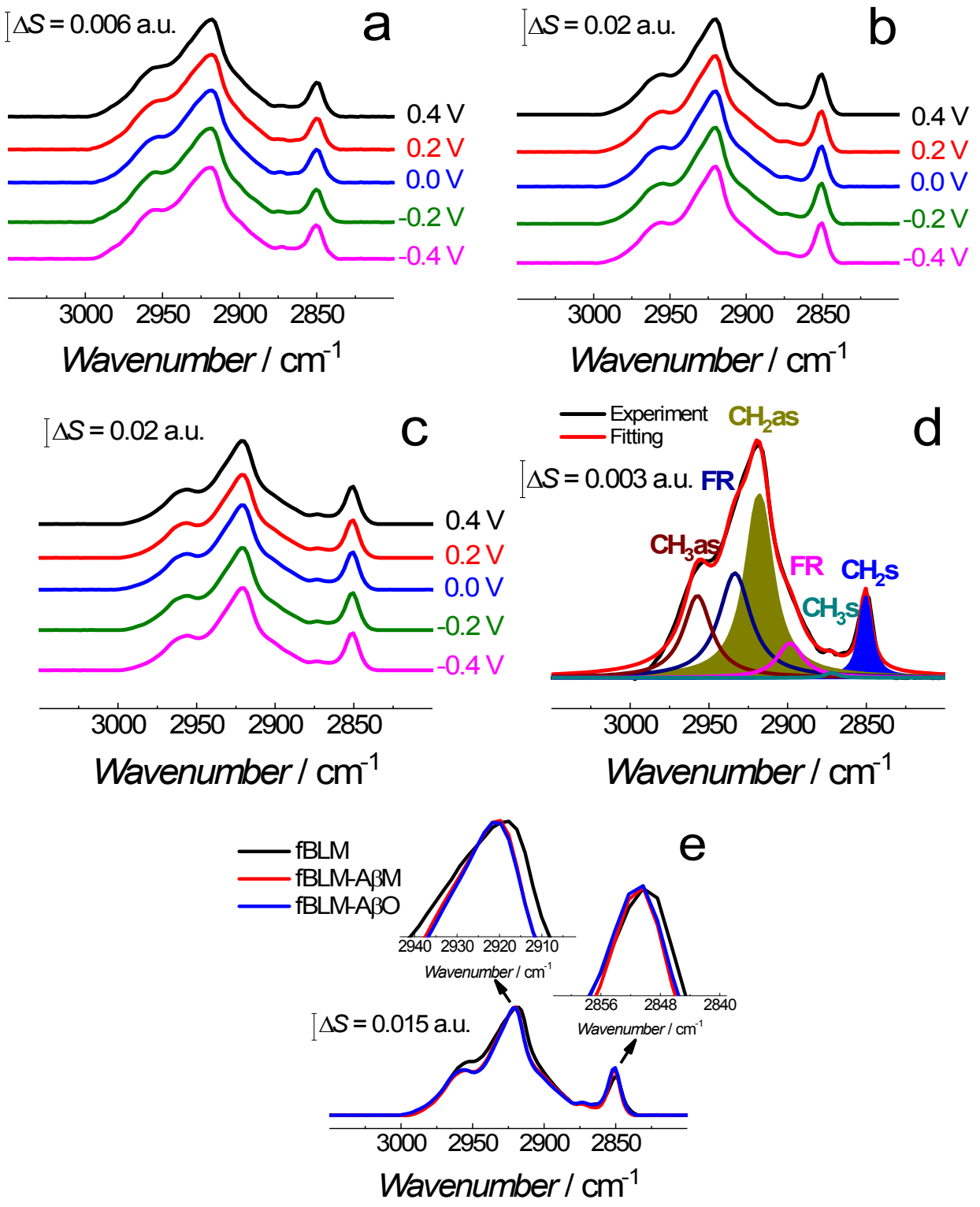

Figure S5. The PM-IRRAS spectra in the C-H stretching band region for (a) fBLM, (b) fBLM-AβMs, and (c) fBLM-AβOs at different potentials in the PBS (0.01 M phosphate buffer, 0.0027 M KCl, and 0.137 M NaCl, pH = 7.4) solution. (d) The deconvoluted PM-IRRAS spectra in the C-H stretching band region showing the

methyl asymmetric (CH_3as), methylene asymmetric (CH_2as), methyl symmetric (CH_3s), methylene symmetric (CH_2as), and Fermi resonance (FR) bands. (e) Overlaid PM-IRRAS spectra for the bare fBLM (black curve), fBLM-AβM (red curve), and fBLM-AβO (blue curve) showing the change in the width and position of C-H stretching bands. Insets show magnified spectra regions of CH_2as (top inset) and CH_2as (right inset) bands for clarity.

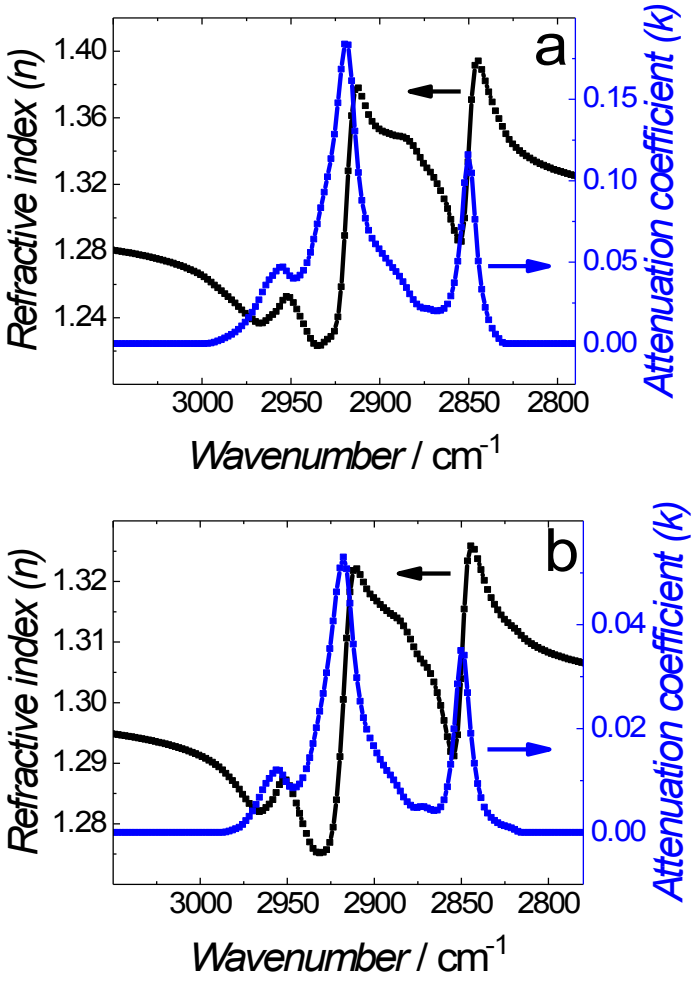

Figure S6. The refractive index and attenuation coefficient dependence on frequency for fBLM vesicles in the (a) absence and (b) presence of AβOs in the PBS/D_2O (0.01 M phosphate buffer, 0.0027 M KCl, and 0.137 M NaCl, pH = 7.4) solution.

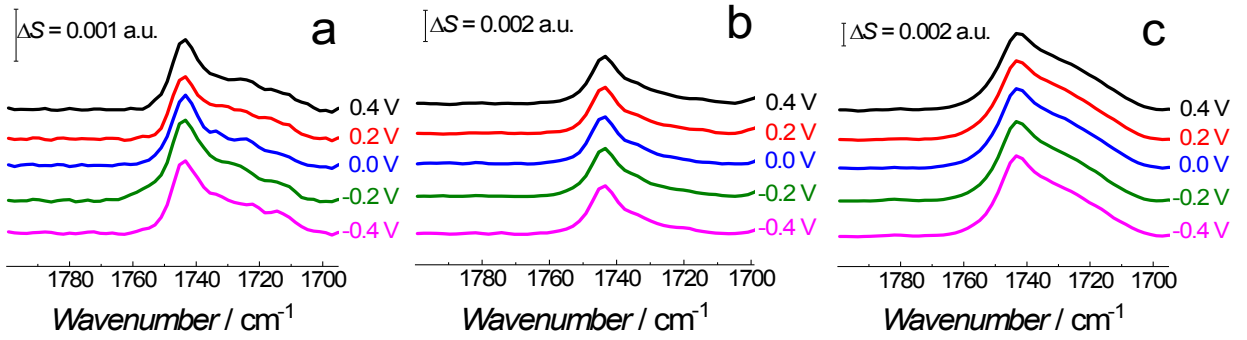

Figure S7. The PM-IRRAS spectra in the C=O stretching band region for (a) fBLM, (b) fBLM-AβMs, and (c) fBLM-AβOs at different potentials in the PBS/D_2O (0.01 M phosphate buffer, 0.0027 M KCl, and 0.137 M NaCl, pH = 7.4) solution.

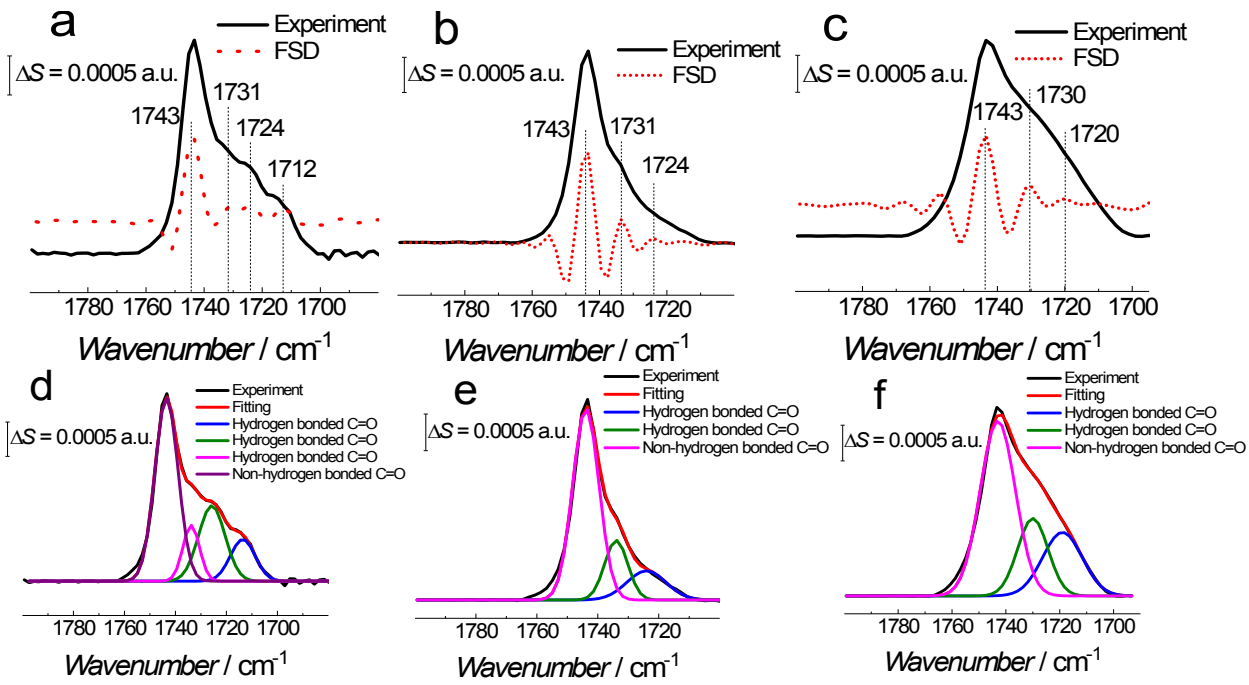

Figure S8. The PM-IRRAS spectra (black solid curves) and corresponding Fourier self-deconvolution (FSD) spectra (red dotted curves) of the C=O band region for (a) fBLM, (b) fBLM-AβMs, and (c) fBLM-AβOs in the PBS/D_2O (0.01 M phosphate buffer, 0.0027 M KCl, and 0.137 M NaCl, pH = 7.4) solution at different potentials. The PM-IRRAS spectra deconvoluted in the C=O band region for (d) fBLM, (e) fBLM-AβMs, and (f) fBLM-AβOs.

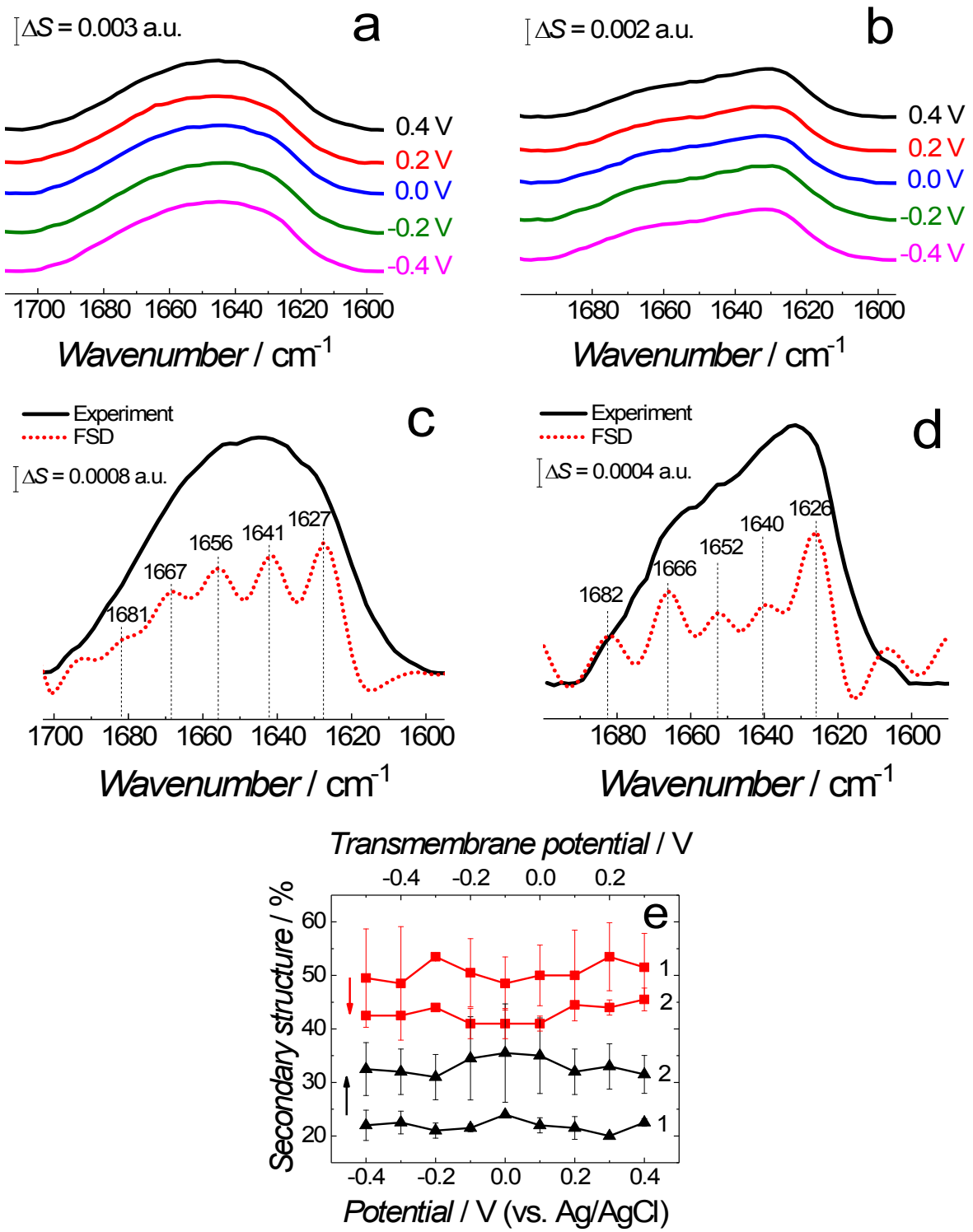

Figure S9. The PM-IRRAS spectra in the amide I band region for (a) fBLM-AβMs and (b) fBLM-AβOs in the PBS/D_2O (0.01 M phosphate buffer, 0.0027 M KCl, and 0.137 M NaCl, pH = 7.4) solution at different potentials. The PM-IRRAS spectra (black solid curves) and the corresponding FSD spectra (red dotted curves) in the amide I band region for (c) fBLM-AβMs and (d) fBLM-AβOs at 0 V vs. Ag/AgCl. The (e) β-

sheet (black curves) and random coil/α-helix (red curves) secondary structure content, estimated by deconvolution of the PM-IRRAS spectra of fBLM-AβM (curve 1) and fBLM-AβO (curve 2) vs. potential. The black arrow indicates an increase in the β-sheet content and the red arrow indicates a decrease in the content of the random coil/α-helix secondary structures in fBLM-AβO compared to corresponding contents in fBLM-AβM.